Inorg. Chem. **2004**, *43*, 7180–7186

New Ligand Systems Incorporating Two and Three 4,4′-Bipyridine Units. Characterization of Bi- and Trimetallic Rhodium and Iridium Complexes

Reto Dorta,[†] Romano Dorta,[‡] Linda J. W. Shimon,[§] and David Milstein*,[†]

Department of Organic Chemistry and Unit of Chemical Research Support, The Weizmann Institute of Science, Rehovot, 76100, Israel, and Departamento de Química, Universidad Simón Bolívar, Caracas 1080A, Venezuela

Received June 1, 2004

The synthesis of new ligand systems based on the bipyridine unit for bi- and trimetallic complexes, including a rare example of a chiral bimetallic complex, is presented. Ligands BBPX (*bi*s-*bip*yridine-*x*ylene, **3**) and TBPBX (*tri*s-*bip*yridine-*bi*s-*x*ylene, **4**) were prepared in one step by reacting α,α′-dibromo-*o*-xylene (**2**) with 2 equiv of the monolithiated derivative of 4,4′-dimethyl-2,2′-bipyridine. Dilithium (*S*)-binaphtholate (**5**) reacted with 2 equiv of 4-bromomethyl-4′-methyl-2,2′-bipyridine (**6**), affording ligand (*S*)-BBPBINAP (*bi*s-*bip*yridine-*binap*htholate, **7**). These ligands reacted cleanly with 1, 1.5, and 1 equiv of the rhodium dimer $[Rh_2Cl_2(HD)_2]$ (HD = 1,5-hexadiene), respectively. Chloride abstraction led to the isolation of the cationic complexes BBPX$[Rh(HD)BF_4]_2$ (**8**), TBPBX$[Rh(HD)BF_4]_3$ (**10**), and (*S*)-BBPBINAP$[Rh(HD)BF_4]_2$ (**12**). When BBPX (**3**), TBPBX (**4**), and (*S*)-BBPBINAP (**7**) were added to 2, 3, and 2 equiv of $[Rh(NBD)_2]BF_4$ or $[Rh(NBD)(CH_3CN)_2]BF_4$ (NBD = norbornadiene), respectively, clean formation of BBPX$[Rh(NBD)BF_4]_2$ (**9**), TBPBX$[Rh(NBD)BF_4]_3$ (**11**), and (*S*)-BBPBINAP$[Rh(NBD)BF_4]_2$ (**13**) was observed. The neutral iridium complex (*S*)-BBPBINAP$[IrCl(COD)]_2$ (**14**) was obtained by reaction of (*S*)-BBPBINAP (**7**) with 1 equiv of $[Ir_2Cl_2(COD)_2]$ (COD = cyclooctadiene). The complexes were fully characterized including X-ray structural studies of **8**, **9**, and **13**, and preliminary studies on their catalytic activity were performed.

Introduction

Soluble transition-metal catalysts are extensively used in industrial and laboratory processes.[1] Cooperative reactivity between multiple metal centers is commonly postulated for enzymatic systems as well as for heterogeneous catalysts and has evolved into an intriguing design principle for synthetic catalysts.[2] Thus, polynucleating ligands that form homo- or heteropolynuclear transition-metal complexes with well-defined geometries are of considerable interest for the development of new supramolecular systems for catalysis, light-to-energy conversion, and molecular devices.[3] Bi- or polymetallic cooperativity in catalytically active complexes has indeed been shown to enhance the selectivity and/or activity of the catalyst, notably in homobimetallic systems.[4] There are still only very few well-characterized chiral bimetallic systems known. In the case of the catalytic enantioselective allylation of aldehydes, Maruoka et al. proposed the in situ formation of chiral bimetallic Ti[5,6] and Zr[7] complexes in order to explain the improved reactivities and selectivities when compared to analogous monomeric complexes. In our laboratories, we have recently shown that the two-dimensional arrangement of a catalyst on a surface leads to cooperative effects in catalytic transformations.[8] Cooperativity is indicated also by a computational study.[9]

* Corresponding author. E-mail: david.milstein@weizmann.ac.il.
† The Weizmann Institute of Science.
‡ Universidad Simón Bolívar.
§ Unit of Chemical Research Support, The Weizmann Institute of Science.

(1) *Homogeneous Catalysis*; Parshall, G. W., Eds.; Wiley: New York, 1980.
(2) (a) *Catalysis by Di- and Polynuclear Metal Cluster Complexes*; Adams, R. A., Cotton, F. A., Eds.; Wiley-VCH: New York, 1998. (b) Braunstein, P.; Rosé, J. In *Metal Clusters in Chemistry*; Braunstein, P., Oro, L. A., Raithby, P. R., Eds.; Wiley-VCH: Weinheim, Germany, 1999; p 616.
(3) (a) Youinou, M.-T.; Rahmouni, N.; Fischer, J.; Osborn, J. A. *Angew. Chem., Int. Ed. Engl.* **1992**, *31*, 733−735. (b) Lehn, J.-M. *Supramolecular Chemistry: Concepts and Perspectives*, VCH: Weinheim, 1995; Chapter 9. (c) Schubert, U. S.; Eschbaumer, C. *Angew. Chem., Int. Ed.* **2002**, *41*, 2892−2926. (c) Holliday, B. J.; Ulmann, P. A.; Mirkin, C. A.; Stern, C. L.; Zakharov, L. N.; Rheingold, A. L. *Organometallics* **2004**, *23*, 1671−1679 and references therein.
(4) Representative examples: (a) Broussard, M. E.; Juma, B.; Train, S. G.; Peng, W.-J.; Laneman, S. A.; Stanley, G. G. *Science* **1993**, *260*, 1784−1788. (b) Konsler, R. G.; Karl, J.; Jacobsen, E. N. *J. Am. Chem. Soc.* **1998**, *120*, 10780−10781. (c) Cai, L.; Mahmoud, H.; Han, Y. *Tetrahedron: Asymmetry* **1999**, *10*, 411−427. (d) He, C.; Lippard, S. J. *J. Am. Chem. Soc.* **2000**, *122*, 184−185 (e) Torres, F.; Sola, E.; Elduque, A.; Martinez, A. P.; Lahoz, F. J.; Oro L. A.; *Chem. Eur. J.* **2000**, *6*, 2120−8.
(5) Hanawa, H.; Hashimoto, T.; Maruoka, K. *J. Am. Chem. Soc.* **2003**, *125*, 1708−1709.
(6) Kii, S.; Maruoka, K. *Tetrahedron Lett.* **2001**, *42*, 1935−1939.
(7) Hanawa, H.; Kii, S.; Asao, N.; Maruoka, K. *Tetrahedron Lett.* **2000**, *41*, 5543−5546.

10.1021/ic049285x CCC: $27.50
Published on Web 09/29/2004

Scheme 1

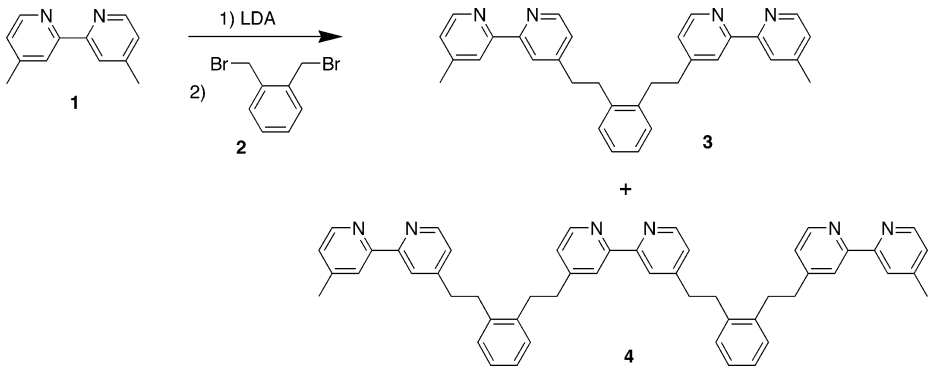

Herein, we wish to report our efforts in the study of novel bi- and trimetallic M(bpy) (bpy = bipyridine, M = Rh, Ir) systems.[10] Bipyridine systems have been studied as catalysts in the hydrogenation of olefins and ketones,[11] and their ability to show cooperative effects has been reported by us.[8] Furthermore, they have received much attention recently as efficient catalysts for the borylation of arenes.[12] We thus prepared three new ligand systems, one of which is chiral, that are capable of chelating two and three metal centers. We report our findings regarding the reactivity of the new ligands BBPX (*b*is-*bip*yridine-*x*ylene, **3**), TBPBX (*t*ris-*bip*yridine-*b*is-*x*ylene, **4**), and (*S*)-BBPBINAP (*b*is-*bip*yridine-*binap*htholate, **7**) toward Rh(I) and Ir(I) metal precursors leading to the isolation of the corresponding homobi- and homotrimetallic complexes. Full characterization of the complexes included X-ray crystallographic analyses of three of them, showing varying metal-to-metal distances in the solid-state, reflecting the relative rigidity of the ligand backbones.

Results and Discussion

Synthesis of the Ligands BBPX (3), TBPBX (4), and (*S*)-BBPBINAP (7). The synthesis of the new ligand systems **3** and **4** was accomplished in one step using commercially available 4,4′-dimethyl-2,2′-bipyridine (**1**) and α,α′-dibromo-*o*-xylene (**2**) as shown in Scheme 1. One of the methyl positions of **1** was lithiated using LDA (lithiumdiisopropylamide, prepared in situ) and subsequently slowly added at −78 °C to a THF solution containing 0.5 equiv of **2**. The solution was left to reach room temperature under stirring, and subsequent workup gave two products as well as unreacted 4,4′-dimethyl-2,2′-bipyridine (**1**) (by TLC). Column chromatography on deactivated silica resulted in the isolation of these three fractions. The first fraction contained unreacted **1**, followed by the desired bis-bipyridine ligand BBPX (**3**), in 38% yield, and the ligand containing three bipyridine units, called TBPBX (**4**), in 15% yield. The isolation of unconsumed reactant **1** and the formation of ligand **4** seem to arise from the poor selectivity in the initial monolithiation process of 4,4′-dimethyl-2,2′-bipyridine. Characterization of **3** and **4** by mass spectrometry showed clearly the expected molecular peaks at 471.3 [M^+] (for **3**) and 757.5 [M^+] (for **4**), respectively. The ^{1}H NMR of ligand **3** gave five signals in the aromatic region for the bipyridine unit, the four protons α to the pyridine giving rise to a single doublet signal at δ = 8.50 ppm. The xylene backbone showed one broad signal for the aromatic protons and a broad signal at δ = 2.96 ppm for all eight protons of the ethylene bridges. The ^{1}H NMR pattern of **4** was similar to that of **3** but gave only four distinguishable signals for the three bipyridine units, with the α and β protons (6 H each) of the bipyridine moieties giving rise to a doublet and a multiplet, respectively.

The synthesis of (*S*)-BBPBINAP (**7**) was accomplished in one step by adding dilithiumbinaphtholate (**5**) to 4-bromomethyl-4′-methyl-2,2′-bipyridine (**6**),[13] in a THF solution and stirring at room temperature for 48 h (eq 1). Hydrolysis and recrystallization from methanol, followed by purification over basic deactivated alumina, gave ligand **7** in 65% yield. The ^{1}H NMR spectrum shows a characteristic AB quartet at 4.81 ppm of the methylene ether protons.

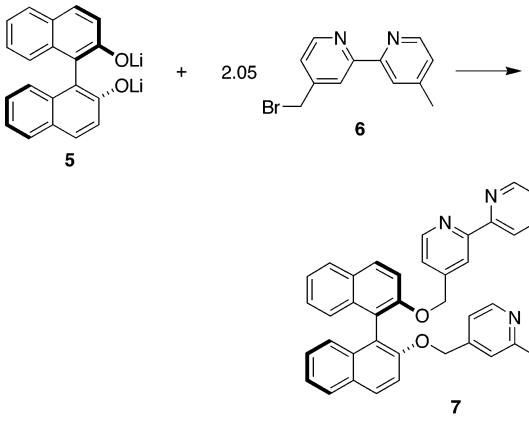

(1)

Formation of Rh(I) and Ir(I) complexes. The ligands **3**, **4**, and **7** reacted cleanly with a series of Rh(I) and Ir(I)

(8) Toellner, K.; Popovitz-Biro, R.; Lahav, M.; Milstein, D. *Science* **1997**, *278*, 2100−2103.

(9) For a computational study of a model of this system, see: Iron, M. A.; Sundermann, A.; Martin J. M. L. *J. Am. Chem. Soc.* **2003**, 125, 11430−11441.

(10) For a recent review dealing with bipyridine ligands and their complexation behavior, see: Kaes, C.; Katz, A.; Hosseini, M. W. *Chem. Rev.* **2000**, *100*, 3553−3590.

(11) For the use of cationic rhodium systems in hydrogenation and hydrogen transfer reactions of olefins and ketones, see: (a) Mestroni, G.; Zassinovich, G.; Camus, A. *J. Organomet. Chem.* **1977**, *140*, 63−72. (b) Mestroni, G.; Spogliarich, R.; Camus, A.; Martinelli, F.; Zassinovich, G. *J. Organomet. Chem.* **1978**, *157*, 345−352. (c) Zassinovich, G.; Mestroni, G.; Gladiali, S. *Chem. Rev.* **1992**, *92*, 1051−1069.

(12) (a) Ishiyama, T.; Takagi, J.; Ishida, K.; Miyaura, N.; Anastasi, N. R.; Hartwig, J. F. *J. Am. Chem. Soc.* **2002**, *124*, 390−391. (b) Ishiyama, T.; Takagi, J.; Hartwig, J. F.; Miyaura, N. *Angew. Chem., Int. Ed.* **2002**, *41*, 3056−3058.

(13) For the synthetic procedure of **6**, see ref 14.

Scheme 2

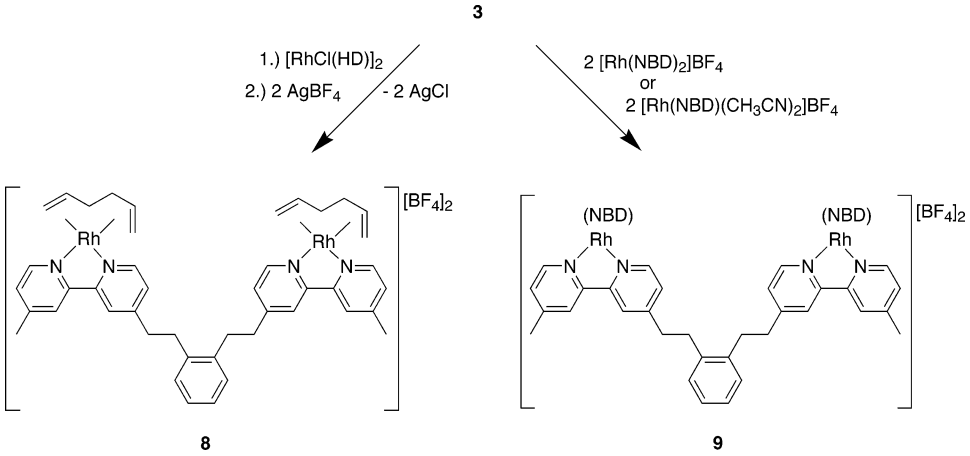

precursors. Ligand **3** reacted with three different Rh(I) precursors according to Scheme 2.

Treatment of 1 equiv of the rhodium dimer $[RhCl(HD)]_2$ (HD = hexadiene; the complex was obtained in situ from $[RhCl(COE)_2]_2$ and excess HD in a methanol solution) with **3** formed an intermediate complex. Subsequent in situ treatment with stoichiometric amounts of $AgBF_4$ to abstract the chloride ligands led to the clean formation of complex $BBPX[Rh(HD)BF_4]_2$ (**8**). The bimetallic complex **8** displays characteristic signals in the ^1H NMR. The ethylene bridges of the diene give rise to two doublet signals with coupling constants to the olefinic proton of 7−8 Hz (for the ones cis to the double bond) and 13−14 Hz (for the hydrogens trans to the double bond). Elemental analysis confirmed the composition of **8**, and in order to unambiguously ascertain the exact structure of this complex, crystals suitable for an X-ray crystallographic analysis were grown by slow diffusion of diethyl ether into a concentrated dichloromethane solution containing **8**. The crystal consists of discrete $BBPX[Rh(HD)^+]_2$ dications, BF_4^- counterions, and one dichloromethane solvent molecule. An ORTEP view of the cationic complex with the atomic numbering scheme is shown in Figure 1 and selected bond distances and angles are found in Table 1.

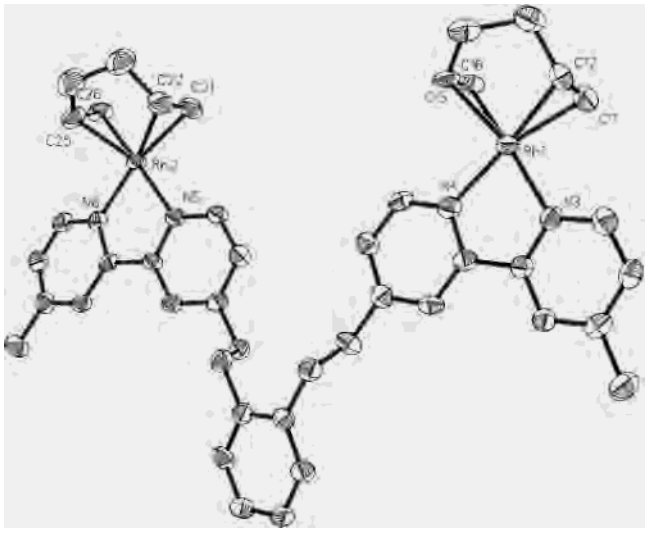

Figure 1. ORTEP diagram of complex **8**. Thermal ellipsoids are drawn at 50% probability. Hydrogen atoms, solvent molecules, and anions are omitted for clarity. See Table 1 for selected bond distances and angles.

Table 1. Selected Bond Distances (Å) and Bond Angles (deg) for Complexes **8**, **9**, and **13**

complex **8**		complex **9**		complex **13**	
Rh1−N4	2.088(5)	Rh1−N1	2.063(2)	Rh1−N6	2.077(4)
Rh1−N3	2.109(5)	Rh1−N2	2.076(2)	Rh1−N5	2.086(5)
Rh1−C16	2.132(6)	Rh1−C44	2.117(3)	Rh1−C13	2.107(6)
Rh1−C11	2.135(7)	Rh1−C41	2.125(3)	Rh1−C14	2.125(5)
Rh1−C15	2.142(6)	Rh1−C43	2.133(2)	Rh1−C16	2.125(6)
Rh1−C12	2.161(7)	Rh1−C42	2.135(3)	Rh1−C11	2.130(6)
Rh2−N6	2.081(5)	Rh2−N3	2.059(2)	Rh2−N7	2.077(4)
Rh2−N5	2.106(5)	Rh2−N4	2.068(2)	Rh2−N8	2.098(5)
Rh2−C25	2.132(7)	Rh2−C54	2.125(3)	Rh2−C21	2.121(6)
Rh2−C21	2.133(6)	Rh2−C53	2.125(3)	Rh2−C22	2.123(6)
Rh2−C26	2.146(6)	Rh2−C52	2.129(3)	Rh2−C25	2.131(6)
Rh2−C22	2.157(7)	Rh2−C51	2.131(2)	Rh2−C24	2.134(6)
N4−Rh1−N3	78.37(19)	N1−Rh1−N2	79.03(9)	N6−Rh1−N5	79.05(18)
N6−Rh2−N5	79.12(18)	N3−Rh2−N4	79.02(8)	N7−Rh2−N8	78.72(17)
Rh1···Rh2	11.73	Rh1···Rh2	7.72	Rh1···Rh2	7.58

The two Rh atoms are in a square planar arrangement with the two cis nitrogen atoms of the bipyridine molecules acting as bidentate chelating ligands. As in complex **9** (see below), the N−Rh distances of the two pyridyl moieties bound to the xylene backbone are slightly shorter than the corresponding N−Rh distances of the "terminal" pyridyls. The Rh−olefin distances are also slightly different with the terminal C−Rh distances (i.e. the CH_2═CHR carbon) being somewhat shorter. The parallel arrangement of ligand BBPX (**3**) in the solid state gave rise to a large Rh···Rh separation of 11.78 Å, most probably leading to a favorable crystal packing between individual molecules of **8**.

Likewise, **3** was reacted with 2 equiv of $[Rh(NBD)_2]BF_4$ or $[Rh(NBD)(CH_3CN)_2]BF_4$ at room temperature, forming the bright orange bimetallic complex $BBPX[Rh(NBD)BF_4]_2$ (**9**) (see Scheme 2). Signals in the ^1H NMR include one set of peaks for the NBD protons and the characteristic pattern in the aromatic region due to the resonances of the bipyridine protons. The molecular structure of **9** was confirmed by an X-ray diffraction study of orange single crystals obtained by slow diffusion of diethyl ether into a concentrated acetone solution containing **9**. An ORTEP drawing of **9** with the atomic numbering scheme is shown in Figure 2 with averages of selected bond distances and angles given in Table 1. The two rhodium atoms are located in a square planar arrange-

Scheme 3

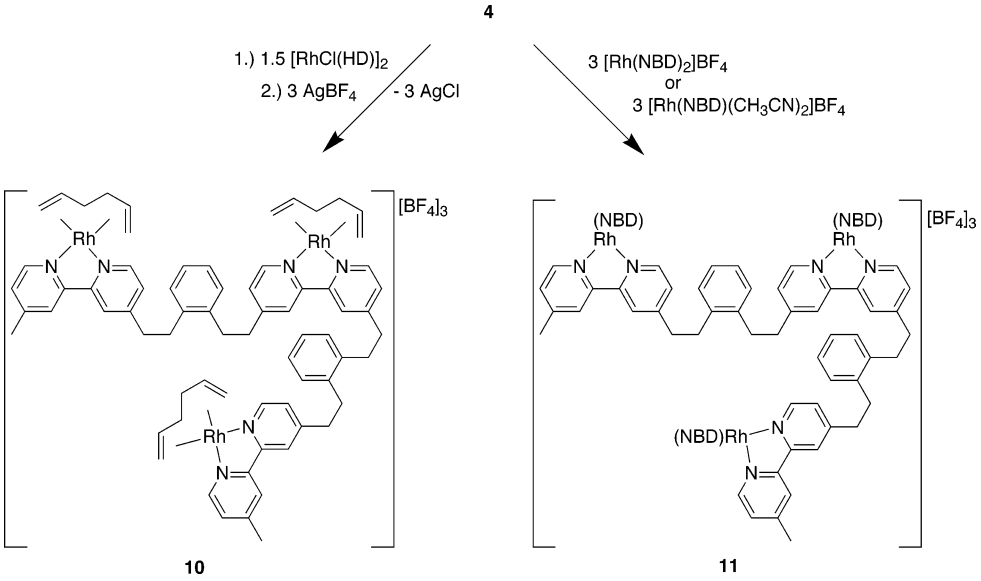

ment with the two double bonds of the dienes trans to the corresponding pyridine moieties. Bond lengths and angles are almost identical to those observed in the bimetallic complex BBPC[Rh(NBD)BF_4]$_2$ (BBPC = *b*is-*bip*yridine-*c*alix[4]arene).[14] The different arrangement of the ligand BBPX compared to complex **8** (in the case of **9**, it is tilted and not parallel) leads to a shorter distance between the two metal centers with a Rh···Rh separation of 7.72 Å. We thus clearly see that the xylene backbone of ligand BBPX is rather flexible, adopting different orientations in the *solid state*.

The coordination chemistry of the TBPBX ligand (**4**) is outlined in Scheme 3. Following the same protocol as for the synthesis of complex **8** but using 1.5 equiv of the starting compound [RhCl(COE)$_2$]$_2$ leads to formation of the trimetallic orange complex TBPBX[Rh(HD)BF_4]$_3$ (**10**). Reaction of **4** with 3 equiv of either [Rh(NBD)$_2$]BF_4 or [Rh(NBD)(CH$_3$CN)$_2$]BF_4 gives the trimetallic, bright orange compound TBPBX[Rh(NBD)BF_4]$_3$ (**11**). The ^{1}H NMR spectra of both these compounds show the expected peaks and equivalent shifts for the three hexadiene (for **10**) and NBD (for **11**) units. Their composition was also confirmed by elemental analysis.

The chiral ligand **7** reacted with Rh(I) and Ir(I) precursors as outlined in Scheme 4. Using the same protocol as for the synthesis of complex **8**, the corresponding chiral bimetallic Rh−hexadiene complex [Rh$_2$(HD)$_2$(*S*)-BBPBINAP][BF_4]$_2$ (**12**) was formed in 78% yield starting from [RhCl(COE)$_2$]$_2$. Ligand **7** also reacted cleanly with [Rh(NBD)$_2$]BF_4 in CD$_3$CN solution to afford complex [Rh$_2$(NBD)$_2$(*S*)-BBPBINAP][BF_4]$_2$ (**13**) as a deep red powder in 75% isolated yield. Complexation of [IrCl(COD)]$_2$ with **7** resulted in almost quantitative formation of the saturated, neutral, deep-blue compound [Ir$_2$Cl$_2$(COD)$_2$((*S*)-BBPBINAP)] (**14**). These compounds were unambiguously characterized by NMR spectroscopy and elemental analysis.

Furthermore, crystals of **13** suitable for an X-ray analysis were grown from a saturated CH$_3$CN solution, affording orange needles. Figure 3 shows an ORTEP representation of **13**, and relevant bond lengths and angles can be found in Table 1. The crystal consists of discrete (*S*)-BBPBINAP-[Rh(NBD)$^+$]$_2$ dications, BF_4^- counterions, and one acetonitrile solvent molecule. The dihedral angle of the (*S*)-binaphthyl unit is 63.44°, within the range of other published binaphthyl substructures. The coordination environment of the two Rh centers is square planar, and the two bipyridyl ligand units are twisted toward each other, bringing the two Rh(NBD) units into rather close diagonal proximity. The Rh(1)−Rh(2) distance of 7.58 Å seems to be determined by van der Waals repulsion of the two NBD ligands. Under hydrogenation conditions, and thus in absence of the NBD ligands, closer contacts between the Rh centers might be possible.

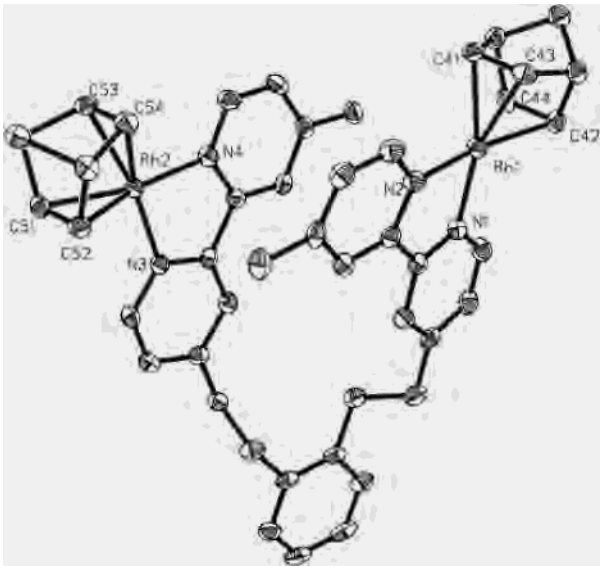

Figure 2. ORTEP diagram of complex **9**. Thermal ellipsoids are drawn at 50% probability. Hydrogen atoms, solvent molecules, and anions are omitted for clarity. See Table 1 for selected bond distances and angles.

(14) Dorta, R.; Shimon, L. J. W.; Rozenberg, H.; Ben-David, Y.; Milstein, D. *Inorg. Chem.* **2003**, *42*, 3160−3167.

Scheme 4

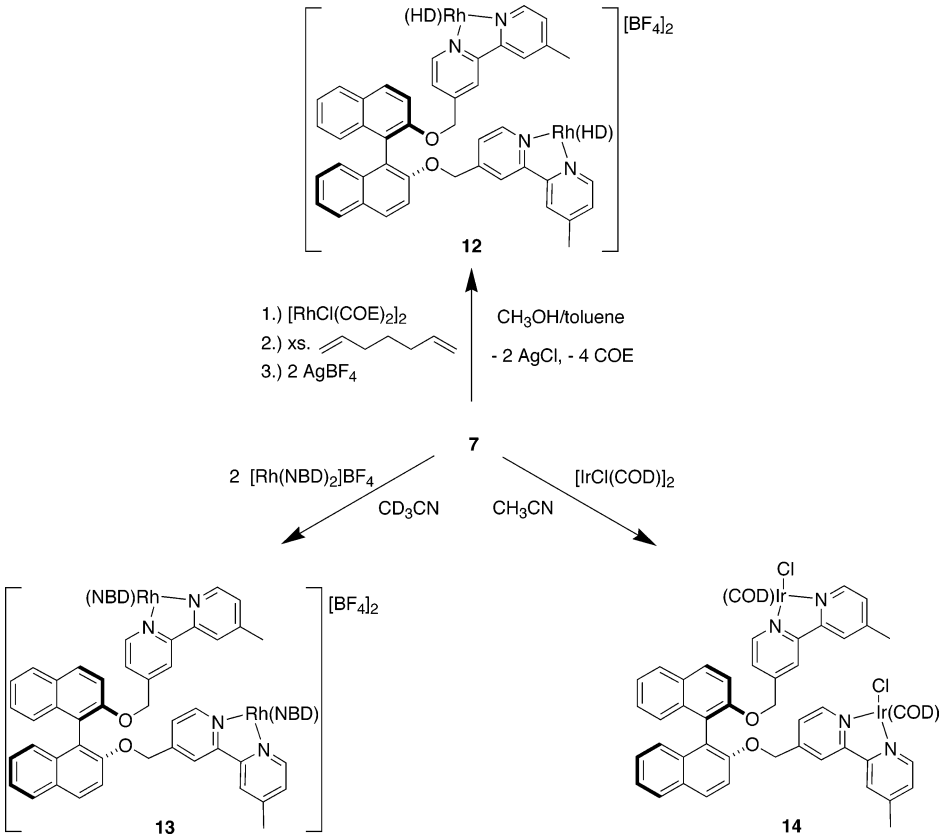

We have performed preliminary hydrogenation experiments using different olefins and ketones employing complexes **8** and **9**, showing that indeed they are active catalysts for the hydrogenation of simple olefins. Catalysis of ketone hydrogenation is very slow under the standard conditions used, i.e., without addition of base. More extensive studies employing the complexes described herein, especially a detailed comparison with their monometallic congeners and enantioselective, bimetallic catalysis with ligand **7**, are currently in progress in our laboratory.

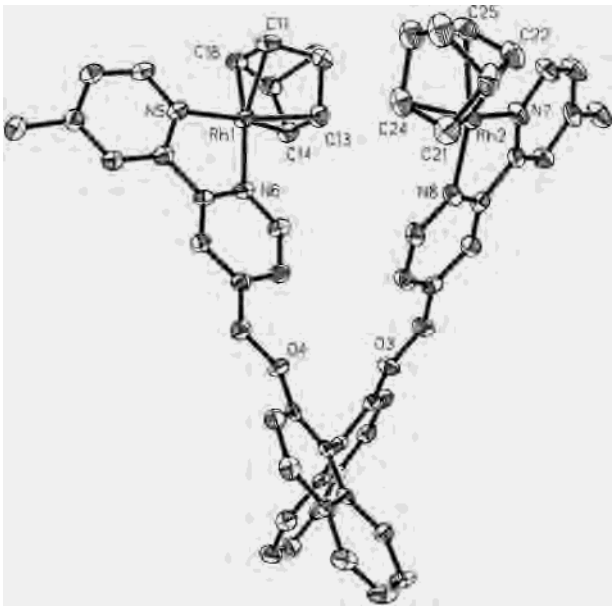

Figure 3. ORTEP diagram of complex **13**. Thermal ellipsoids are drawn at 50% probability. Hydrogen atoms, solvent molecules, and anions are omitted for clarity. See Table 1 for selected bond distances and angles.

Summary

Three new ligand systems based on the chelating bipyridine ligand unit, namely BBPX (**3**), TBPBX (**4**), and chiral (*S*)-BBPBINAP (**7**) were synthesized for the formation of bi- and trinuclear systems. The ligands reacted with Rh(I) and Ir(I) precursors giving the bi- and trimetallic complexes **8**−**14**, which were fully characterized. Furthermore, the structures of three of them, namely BBPX[Rh(HD)BF_4]$_2$ (**8**), BBPX[Rh(HD)BF_4]$_2$ (**9**), and [Rh_2(NBD)$_2${(*S*)-BBPBINAP}]-[BF_4]$_2$ (**13**), were confirmed by X-ray analyses showing metal-to-metal distances of 11.73, 7.72, and 7.58 Å, respectively. The catalytic potential of these polynuclear complexes is currently being studied, and the results will be reported in due course. Furthermore, the applicability of these new ligand systems to the synthesis of new (in the case of ligand **7**, chiral) supramolecular structures is being studied.

Experimental Section

General Procedures. All experiments were carried out under an atmosphere of purified nitrogen in a Vacuum Atmospheres glovebox equipped with a MO 40-2 inert gas purifier. Ligand synthesis was performed using standard Schlenk techniques. All solvents were reagent grade or better. All nondeuterated solvents were refluxed over sodium/benzophenone ketyl and distilled under an argon atmosphere. Deuterated solvents were used as received. All the solvents were degassed with argon and kept in the glovebox over molecular sieves. Commercially available reagents were used

as received. Butyllithium (ca. 1.6 M solution in hexane, Aldrich) was titrated immediately before use. 4-Bromomethyl-4′-methyl-2,2′-bipyridine (**6**) was synthesized according to a literature procedure.[14] The complexes $[Rh_2Cl_2(COE)_4]$,[15] $[Rh(NBD)_2]BF_4$, and $[Rh(NBD)(CH_3CN)_2]BF_4$,[16] were prepared according to literature procedures. ^{1}H and ^{13}C (DEPT) 1D NMR spectra were recorded on a Bruker DPX-250 or a Bruker DRX-400 spectrometer. Measurements were carried out at a probe temperature of 25 °C. Chemical shifts are reported in ppm downfield from tetramethylsilane and are referenced to the residual hydrogen signal of the deuterated solvents (2.04 ppm, acetone; 2.49 ppm, DMSO; 5.32 ppm, dichloromethane, 7.24 ppm, chloroform). Abbreviations used in the description of NMR data are as follows: br, broad; s, singlet; d, doublet; t, triplet; m, multiplet. Elemental analyses were performed by H. Kolbe, Mikroanalytisches Laboratorium, 45470 Mühlheim, Germany.

Synthesis of the Ligands BBPX (3) and TBPBX (4). Diisopropylamine (2.53 g, 25 mmol) was added via syringe to a THF (30 mL) solution and cooled to −78 °C. Butyllithium (17.48 mL, 25 mmol, 1.43 M) was added dropwise via cannula and the temperature was gradually increased to 0 °C. After 10 min at 0 °C, the solution was cooled again to −78 °C. The solution was added dropwise at −78 °C via cannula to a solution of THF (50 mL) containing 2,2′-dimethyl-4,4′-bipyridine (3.87 g, 21 mmol). The resulting deep-red solution was then transferred via cannula at −78 °C to a solution of α,α′-dibromo-*o*-xylene (2.64 g, 10 mmol) in THF (15 mL) at −78 °C. The reaction was left stirring overnight, gradually reaching room temperature. The brown solution was quenched with MeOH (10 mL), giving rise to a color change to yellow. Subsequent extraction with diethyl ether (3 × 250 mL), drying over Na_2SO_4, filtration, and evaporation of the solvent afforded a mixture of three compounds (according to TLC) as a yellowish solid. The crude product was loaded onto a deactivated silica gel column (pretreated with 10% triethylamine in hexane and subsequently washed with hexane) and was eluted with 10% EtOAc/hexane, gradually increasing polarity to 100% EtOAc. The first product coming out was 2,2′-dimethyl-4,4′-bipyridine (15%), followed by BBPX (**3**, 38%) and TBPBX (**4**, 15%). A fourth and last fraction could not be isolated. The products **3** and **4** were further purified by dissolving them in a minimal amount of EtOAc, precipitation with hexane, filtration, and drying in vacuo. **3**: Yield: 1.88 g, 38%. ^{1}H NMR (250 MHz, CD_2Cl_2, 298 K): δ = 2.42 (s, 6 H), 2.97 (s, br, 8 H), 7.06 (d, 5.0 Hz, 2 H), 7.11 (d, 4.9 Hz, 2 H), 7.17 (s, 4 H), 8.19 (s, 2 H), 8.27 (s, 2 H), 8.50 (d, 5.0 Hz, 4 H); $C_{32}H_{30}N_4$: 470.62. MS (EI): *m*/*z* 471.3 [M^+]. **4**: Yield: 795 mg, 15%. ^{1}H NMR (250 MHz, CD_2Cl_2, 298 K): δ = 2.38 (s, 6 H), 2.95 (s, br, 16 H), 7.05 (m, 6 H), 7.15 (s, 8 H), 8.19 (s, br, 2 H), 8.27 (s, br, 4 H), 8.49 (d, 4.9 Hz, 6 H); $C_{52}H_{48}N_6$: 756.99. MS (EI): *m*/*z* 757.5 [M^+].

(*S*)-BBPBINAP (7). A solution of bis-lithium-binaphtholate (1.366 g) in THF (25 mL) was added dropwise to a vigorously stirred solution of 4-bromomethyl-4′-methyl-2,2′-bipyridine (2.453 g) in THF (25 mL). The resulting yellow solution was stirred at room temperature for 72 h, thereby turning darker. The volatiles were then removed under vacuum, yielding a golden glassy solid that was purified by flash chromatography: column dimension, *d* = 4 cm, *l* = 15 cm; stationary phase, basic deactivated alumina (Brockmann IV); eluent, ethyl acetate/hexane = 1/1 with 5 mL NEt_3/L. Removing the volatiles under vacuum gave a white powder. Yield: 1.95 g, 65%. ^{1}H NMR (C_6D_6): δ = 1.94 (s, 6 H), 4.81 (4 H, AB quartet, J_1 = 19 Hz, J_2 = 14 Hz), 6.60−6.70 (m, 2 H), 6.70−6.80 (m, 2 H), 7.10−7.30 (m, 6 H), 7.50−7.60 (m, 2H), 7.70−7.85 (m, 4 H), 8.35−8.45 (m, 2 H), 8.50−8.55 (m, 2 H), 8.55−8.65 (m, 4 H). The spectrum shows the presence of ca. 0.25 mol % of AcOEt. Anal. Calcd for $C_{44}H_{34}N_4O_2$·0.25AcOEt (FW 672.84): C, 80.33; H, 5.40; N, 8.33. Found: C, 80.00; H, 5.65; N, 8.14.

BBPX[Rh(HD)BF$_4$]$_2$ (8). $[Rh_2Cl_2(COE)_4]$ (280 mg, 0.392 mmol, COE = cyclooctene) was dissolved in MeOH (15 mL), and excess HD (HD = 1,5-hexadiene, 2.28 mL) was added dropwise via syringe giving a yellow crystalline solution that was left stirring at room temperature for 30 min. BBPX (**3**) (186 mg, 0.395 mmol) dissolved in CH_2Cl_2 (8 mL) was added dropwise, resulting in a color change to red. The solution was left stirring at room temperature for 4 h before $AgBF_4$ (152.6 mg, 0.784 mmol) in CH_2Cl_2 (5 mL) was added. Stirring the mixture at room temperature for another hour was followed by dilution with additional CH_2Cl_2 (30 mL) and filtration over Celite. The orange-red solution was concentrated in vacuo to 5 mL, and addition of diethyl ether led to the precipitation of complex **8** as an orange-red microcrystalline solid. The solid was filtered, washed with additional diethyl ether, and dried in vacuo. Yield: 161 mg, 87%. ^{1}H NMR (acetone-d_6): δ = 1.91 (m, 4 H), 2.51 (m, 4 H), 2.56 (s, 6 H), 2.96 (d, 13.7 Hz, 4 H), 3.10 (s, 8 H), 3.55 (d, 7.5 Hz, 4 H), 4.75 (m, 4 H), 7.18 (s, 4 H), 7.39 (d, 5.5 Hz, 2 H), 7.46 (d, 5.7 Hz, 2 H), 7.59 (d, 5.6 Hz, 2 H), 7.65 (d, 5.5 Hz, 2 H), 8.26 (s, 4 H). ^{13}C NMR (acetone-d_6, selected): δ = 63.3 (d, 12.1 Hz, *C*H_2-olefin), 91.0 (d, 11.7 Hz, *C*HR-olefin). Anal. Calcd for $C_{44}H_{50}B_2F_8N_4Rh_2$ (FW 1014.37): C, 52.10; H, 4.97; N, 5.52. Found: C, 52.19; H, 5.07; N, 5.46.

BBPX[Rh(NBD)BF$_4$]$_2$ (9). $[Rh(NBD)(CH_3CN)_2]BF_4$ (62 mg, 0.170 mmol) and BBPX (**3**) (40 mg, 0.085 mmol) were dissolved in CH_2Cl_2 (4 mL each), mixed together, and stirred at room temperature for 4 h. Compound **9** was obtained as a deep red microcrystalline solid by precipitation with diethyl ether, washing with diethyl ether, and drying in vacuo. Yield: 61 mg, 92%. ^{1}H NMR (CD_2Cl_2): δ = 1.52 (s, 4 H), 2.52 (s, 6 H), 3.02 (s, br, 8 H), 4.06 (s, 4 H), 4.35 (m, 8 H), 7.16 (s, 4 H), 7.36 (m, 6 H), 7.46 (d, 5.1 Hz, 2H), 8.16 (s, 4 H). Anal. Calcd for $C_{46}H_{46}B_2F_8N_4Rh_2$ (FW 1034.36): C, 53.42; H, 4.49; N, 5.42. Found: C, 53.33; H, 4.38; N, 5.31.

TBPBX[Rh(HD)BF$_4$]$_3$ (10). $[Rh_2Cl_2(COE)_4]$ (140 mg, 0.196 mmol, COE = cyclooctene) was dissolved in MeOH (6 mL), and excess HD (HD = 1,5-hexadiene, 1.14 mL) was added dropwise via syringe, giving a yellow crystalline solution that was left stirring at room temperature for 30 min. TBPBX (**4**) (99 mg, 0.1308 mmol) dissolved in CH_2Cl_2 (6 mL) was added dropwise, resulting in a color change to red. The solution was left stirring at room temperature for 3 h before $AgBF_4$ (76.2 mg, 0.392 mmol) in CH_2Cl_2 (6 mL) was added. Stirring the mixture at room temperature for another hour was followed by dilution with CH_2Cl_2 (10 mL) and filtration over Celite. The orange-red solution was concentrated in vacuo to 8 mL. Addition of diethyl ether led to the precipitation of complex **10** as an orange microcrystalline solid which was filtered, washed with additional diethyl ether, and dried in vacuo. Yield: 88 mg, 89%. ^{1}H NMR (acetone-d_6): δ = 1.90 (m, 6 H), 2.49 (m, 6 H + 6 H), 2.93 (d, 13.8 Hz, 6 H), 3.06 (s, 16 H), 3.52 (d, 6.7 Hz, 6 H), 4.72 (m, 6 H), 7.17 (s, 8 H), 7.38 (d, 5.3 Hz, 2 H), 7.46 (m, 4 H), 7.57 (d, 5.7 Hz, 2 H), 7.63 (d, 5.7 Hz, 4 H), 8.21 (s, 4 H), 8.33 (s, 2 H). ^{13}C NMR (acetone-d_6, selected): δ = 63.3 (m, *C*H_2-olefin), 91.0 (d, 11.6 Hz, *C*HR-olefin), 91.1 (d, 11.6 Hz, *C*HR-olefin). Anal. Calcd for $C_{70}H_{78}B_3F_{12}N_6Rh_3$ (FW 1572.63): C, 53.46; H, 5.00; N, 5.34. Found: C, 53.38; H, 5.06; N, 5.30.

(15) Hofmann, P.; Meier, C.; Englert, U.; Schmidt, U. *Chem. Ber.* **1992**, *125*, 353−365.
(16) Green, M.; Kuc, T. A. *J. Chem. Soc., Dalton Trans.* **1972**, 832−839.

TBPBX[Rh(NBD)BF_4]$_3$ (11). A solution of TBPBX (**4**) (35 mg, 0.046 mmol) in CH_3CN (8 mL) was added dropwise to a solution of [Rh(NBD)$(CH_3CN)_2$]BF_4 (50 mg, 0.139 mmol) in CH_3CN (4 mL). The resulting orange-red solution was stirred at room temperature for 8 h and then concentrated to 4 mL. Slow addition of diethyl ether resulted in precipitation of **11** as a red solid, which was decanted, washed with additional diethyl ether, and dried in vacuo. Yield: 69 mg, 93%. ^{1}H NMR (250 MHz, CD_2Cl_2, 298 K): δ = 1.55 (s, 6 H), 2.48 (s, 6 H), 3.05 (m, 16 H), 4.08 (s, 6 H), 4.36 (m, 12 H), 7.18 (s, 8 H), 7.36 (m, 8 H), 7.44 (d, 5.5 Hz, 4H), 8.15 (s, 4 H), 8.30 (s, 2 H). Anal. Calcd for $C_{73}H_{72}B_3F_{12}N_6Rh_3$ (FW 1602.61): C, 54.71; H, 4.53; N, 5.24. Found: C, 54.88; H, 4.62; N, 5.29.

Note*:* Complexes **9** and **11** were also obtained starting from [Rh(NBD)$_2$]BF_4.

(*S*)-BBPBINAP)[Rh(HD)BF_4]$_2$ (12). 1,5-Hexadiene (0.60 mL) was added to a slurry of [RhCl$(COE)_2]_2$ (76.3 mg, 0.107 mmol) in CH_3OH (5 mL), yielding a yellow microcrystalline precipitate upon stirring for 3 h. Then a solution of (*S*)-BBPBINAP (**7**) (69.9 mg, 0.107 mmol) in toluene (2.5 mL) was added dropwise under stirring to afford a deep red solution. Stirring was continued for 3 h. The subsequent addition of a solution of $AgBF_4$ (41.5 mg, 0.213 mmol) in toluene (2.5 mL) caused the precipitation of a grayish solid. This mixture was stirred for another 3 h and filtered over Celite. The filtrate was evaporated to dryness and slurried in Et_2O (5 mL). The resulting solid was filtered off and dried in vacuo, affording a brick-red powder. Yield: 100 mg, 78%. ^{1}H NMR (CD_2Cl_2): δ 1.80−1.95 (m, 4H), 2.40−2.55 (m, 4H), 2.58 (s, 6H), 2.85−3.00 (m, 4H), 3.40−3.55 (m, 4H), 4.50−4.80 (br, 4 H), 5.25−5.45 (m, 4 H), 7.00−7.15 (m, 4H), 7.15−7.30 (m, 2H), 7.30−7.45 (m, 6H), 7.50−7.65 (m, 4H), 7.70−7.95 (m, 6H), 7.95−8.10 (m, 2H). The spectrum indicates the presence of ca. 0.33 mol % Et_2O. Anal. Calcd for $C_{56}H_{54}B_2F_8N_4O_2Rh_2 \cdot 0.33C_4H_{10}O \cdot 3H_2O$ (FW 1273.30): C, 54.08; H, 5.01; N, 4.40. Found: C, 53.76; H, 4.74; N, 3.99.

[Rh_2\{(*S*)-BBPBINAP\}(NBD)$_2$][BF_4]$_2$ (13). A solution of [Rh(NBD)$_2$]BF_4 (33.0 mg, 0.088 mmol) in CD_3CN (0.5 mL) was added dropwise to a slurry of (*S*)-BBPBINAP (7) (28.8 mg, 0.0443 mmol) in CD_3CN (0.5 mL), affording an orange solution after addition of the first equivalent of Rh and turning deep red upon addition of the second equivalent. Stirring overnight caused the precipitation of large amounts of a red solid, which was isolated by filtration and dried in vacuo. Yield: 40 mg, 75%. ^{1}H NMR (DMSO-d_6): δ 1.33 (s, 4 H), 2.46 (s, 6 H), 3.96 (s, 4 H), 4.15 (s, 8 H), 5.21 (d, J = 15 Hz, 2 H), 5.46 (d, J = 15 Hz, 2 H), 6.93 (d, J = 8 Hz), 7.10−7.30 (m, 8 H), 7.40−7.70 (m, 8 H), 7.76 (d, J = 9 Hz, 2 H), 7.91 (d, J = 8 Hz, 2 H), 8.16 (d, J = 9 Hz, 2 H). Anal. Calcd for $C_{58}H_{50}O_2N_4Rh_2B_2F_8 \cdot 3H_2O$ (FW 1268.58): C, 54.92; H, 4.45; N, 4.42. Found: C, 54.94; H, 4.27; N, 4.27.

[Ir_2Cl_2(COD)$_2$((*S*)-BBPBINAP)] (14). A yellow solution of [IrCl$(COD)]_2$ (393.2 mg, 0.5854 mmol) in CH_3CN (6 mL) was added dropwise to a colorless solution of (*S*)-BBPBINAP (385.1 mg, 0.5862 mmol) in CH_3CN (6 mL), immediately causing the formation of a black-blue precipitate. The mixture was stirred overnight. Filtration, washing with Et_2O (2 × 12 mL), and drying in vacuo yielded a dark violet fine powder (760 mg, 97%). ^{1}H NMR ($CDCl_3$): δ 1.65−1.75 (m, 8 H), 2.25−2.40 (m, 8 H), 2.30 (s, 6 H), 3.60−3.70 (m, 8 H), 4.48 (d, J = 15 Hz, 2 H), 4.99 (d, J = 15 Hz, 2 H), 6.70−6.80 (m, 2 H), 7.05−7.15 (m, 2 H), 7.15−7.35 (m, 4 H), 7.35−7.50 (m, 4 H), 7.75−7.85 (m, 2 H), 7.85−8.10 (m, 10 H). Anal. Calcd for $C_{60}H_{58}Cl_2Ir_2N_4O_2$ (FW 1322.32): C, 54.49; H, 4.42; N, 4.24. Found: C, 54.84; H, 4.49; N, 4.11.

X-ray Crystal Structure Determination of 8, 9, and 13. Single crystals of **8**, **9**, and **13** were mounted on a nylon loop and flash frozen in a nitrogen stream at 120 K. Data were collected on a Nonius KappaCCD diffractometer mounted on a FR590 generator equipped with a sealed tube with Mo Kα radiation (λ = 0.71073 Å) and a graphite monochromator. The structures were solved using direct method with SHELXS-97 and refined by full-matrix least-squares technique with SHELXL-97 based on F^2.[17]

Complex 8. $C_{44}H_{50}N_4Rh_2 + 2(BF_4) + CH_2Cl_2$, orange, plates, 0.30 × 0.10 × 0.02 mm^3, monoclinic, $P2(1)/n$, a = 11.213(2) Å, b = 19.493(4) Å, c = 20.205(4) Å, β = 90.52(3)°, V = 4416.1(15) Å^3, Z = 4, FW = 1099.24, D_c = 1.653 Mg/m^3, μ = 0.941 mm^{-1}. The final cycle of refinement based on F^2 gave an agreement factor R = 0.0506 for data with $I > 2\sigma(I)$ and R = 0.0691 for all data (4219 reflections) with a goodness-of-fit of 1.006. Idealized hydrogen atoms were placed and refined in riding mode.

Complex 9. $C_{46}H_{46}N_4Rh_2 + 2(BF_4)$, orange, prisms, 0.30 × 0.10 × 0.10 mm^3, monoclinic, $C2/c$ (No. 15), a = 37.115(7) Å, b = 8.313(2) Å, c = 31.477(6) Å, β = 9120.64(3)°, V = 8356(3) Å^3, Z = 8, FW = 1034.31, D_c = 1.644 Mg/m^3, μ = 0.866 mm^{-1}. The final cycle of refinement based on F^2 gave an agreement factor R = 0.0255 for data with $I > 2\sigma(I)$ and R = 0.0311 for all data (4219 reflections) with a goodness-of-fit of 1.031. Idealized hydrogen atoms were placed and refined in riding mode.

Complex 13. $C_{58}H_{50}N_4O_2Rh_2 + 2(BF_4) + C_2H_3N$, orange, needles, 0.1 × 0.05 × 0.01 mm^3, monoclinic, $P2(1)/n$ (No. 14), a = 12.237(2) Å, b = 16.728(3) Å, c = 25.783(5) Å, α = 90°, β = 98.96(3)°, γ = 90° from 20° of data, V = 5213.4(16) Å^3, Z = 4, FW = 1255.51, D_c = 1.600 Mg/m^3, μ = 0.713 mm^{-1}. The final cycle of refinement based on F^2 gave an agreement factor R = 0.0489 for data with $I > 2\sigma(I)$ and R = 0.0664 for all data (7257 reflections) with a goodness-of-fit of 1.020. Idealized hydrogen atoms were placed and refined in riding mode.

Acknowledgment. This work was supported by the Israel Science Foundation, Jerusalem, Israel, and by the MINERVA foundation, Munich, Germany. D.M. is the Israel Matz Professor of Organic Chemistry.

Supporting Information Available: Tables of crystal and structure refinement data, atomic coordinates, bond lengths and angles, anisotropic displacement parameters, and hydrogen coordinates for complexes **8**, **9**, and **13** in CIF format. This material is available free of charge via the Internet at http//pubs.acs.org.

IC049285X

(17) SHELXL-97, Program for Crystal Structure Refinement, G. M. Sheldrick, University of Göttingen, Göttingen, Germany, 1997.